

# When is settling important for particle concentrations in wall-bounded turbulent flows?

A.D. Bragg<sup>†1</sup>, D. H. Richter<sup>2</sup> and G. Wang<sup>‡3</sup>

<sup>1</sup>Department of Civil and Environmental Engineering, Duke University, Durham, NC 27708, USA

<sup>2</sup>Department of Civil and Environmental Engineering and Earth Sciences, University of Notre Dame, Notre Dame, Indiana 46556, USA

<sup>3</sup>Physics of Fluids Group and Twente Max Planck Center, Department of Science and Technology, Mesa+ Institute, and J. M. Burgers Center for Fluid Dynamics, University of Twente, P.O. Box 217, 7500 AE Enschede, The Netherlands

(Received xx; revised xx; accepted xx)

We explore the role of gravitational settling on inertial particle concentrations in a wall-bounded turbulent flow. While it may be thought that settling can be ignored when the Stokes settling velocity  $v_s$  is small compared with the fluid friction velocity  $u_\tau$ , we show that even in this regime the settling may make a leading order contribution to the concentration profiles. This is because the importance of settling is determined, not by the size of  $v_s$  compared with  $u_\tau$  or any other fluid velocity scale, but by its size relative to the turbophoretic drift velocity. We explain this in the context of the particle mean-momentum equation, and show that in general, there always exists a region in the boundary layer where settling cannot be neglected, no matter how small  $v_s/u_\tau$  is (provided it is finite). Direct numerical simulations confirm the arguments, and show that even for  $v_s/u_\tau = O(10^{-2})$ , the near wall particle concentration can be orders of magnitude larger than for the case where  $v_s/u_\tau = 0$ , and for  $v_s/u_\tau = O(10^{-3})$  enhancements of up to a factor of two are observed. For weakly inertial particles, it is found that even for  $v_s/u_\tau = O(10^{-2})$ , the preferential sampling of ejection events in the boundary layer by the inertial particles is profoundly modified compared with the  $v_s/u_\tau = 0$  case.

## 1. Introduction

In many particle-laden, wall-bounded turbulent flows, it is important to characterize the near-wall distribution of a dispersed phase. In the environment, surface emission of particulate matter (e.g. dust, aerosols) is often estimated by assuming a relationship between the mean concentration and surface flux. This flux-profile relationship is also the basis for wall models of heavy scalar transport (Chamecki *et al.* 2009).

While many past studies have focused on the phenomena of turbophoresis (Reeks 1983) and the interactions of particles with near-wall coherent structures (Soldati & Marchioli 2009), much less attention has been given to the settling of particles through wall-bounded turbulence. And while it is well-known that particles can experience an inertial enhancement to their settling velocity in isotropic, homogeneous turbulence (Maxey 1987), the interplay between settling and inertial effects, especially near the wall, is much less understood. Due to the existence of gradients of particle concentration

<sup>†</sup> Email address for correspondence: andrew.bragg@duke.edu

<sup>‡</sup> Email address for correspondence: g.wang@utwente.nl

and turbulence kinetic energy near the wall, the balance between the various mechanisms of particle drift have not been fully explored.

In this regard, it is common to neglect the effects of gravity despite the presence of finite inertia, as long the particle settling velocity is deemed sufficiently small. The relevant nondimensional parameter which describes this, however, is often assumed to be the ratio of the particle settling velocity  $\tau_p g$  (where  $\tau_p$  is the particle response time and  $g$  is the gravitational acceleration) to the flow friction velocity  $u_\tau$ . What we aim to demonstrate both theoretically and numerically, however, is that near the wall, even small Stokes settling velocities can be comparable in magnitude to the turbophoretic (i.e. inertial) drift velocities. This in turn disrupts commonly assumed balances which ultimately determine the wall-normal distribution of particles, such as the well-known theory of Rouse (1937) which predicts a power-law distribution of a heavy scalar.

## 2. Theory and analysis

We consider the vertical motion of small, heavy particles subject to Stokes drag and gravitational forces (Maxey & Riley 1983)

$$\frac{d}{dt}w^p(t) = \frac{1}{\tau_p} \left( u^p(t) - w^p(t) \right) - g, \quad (2.1)$$

where  $w^p(t)$  is the vertical particle velocity and  $u^p(t)$  is the vertical fluid velocity at the particle position.

In assessing the importance of gravitational settling on particle motion in turbulent flows, it is typical to define a settling parameter such as  $\tau_p g/u_\eta$  (Balachandar 2009, where  $u_\eta$  is the Kolmogorov velocity scale) or in the context of boundary layers  $\tau_p g/u_\tau$  (Johnson *et al.* 2020), and then to conclude that the effect of settling can be neglected when these non-dimensional parameters are small. Nevertheless, in some works, the effect of gravitational settling has been shown to be important even when such parameters are small. For example, DNS results in Richter & Chamecki (2018) and Bragg *et al.* (2020) showed that even when  $\tau_p g/u_\tau = O(10^{-2})$ , the effect of gravitational settling on the particle motion in the boundary layer was strong, and in some parameter regimes, made a leading order contribution to the particle motion. As we will now show, this is because quantities such as  $\tau_p g/u_\tau$  are inappropriate measures of the importance of settling on the particle motion in the boundary layer.

Using phase-space Probability Density Function (PDF) equations, we can construct transport equations for the average particle spatial distribution  $\varrho \equiv \langle \delta(z^p(t) - z) \rangle$ , where  $z^p(t)$  is the vertical particle position,  $z$  is the time-independent vertical position coordinate (with  $z = 0$  corresponding to the wall), and  $\langle \cdot \rangle_z$  denotes an ensemble average conditioned on  $z^p(t) = z$ . We normalize all quantities using the fluid friction timescale  $\tau$  and velocity scale  $u_\tau$  to express them in wall units, usually denoted by the superscript  $+$ . However, in what follows, we drop the superscript for notational simplicity. Then, for a fully developed wall-bounded turbulent flow, with zero average particle mass-flux, the mean-momentum equation reduces to (Bragg *et al.* 2020)

$$0 = -StS\nabla_z \varrho + \varrho \langle u^p(t) \rangle_z - St\varrho \nabla_z S - Sv\varrho, \quad (2.2)$$

where  $S \equiv \langle (w^p(t) - \langle w^p(t) \rangle_z)^2 \rangle_z$  is the variance of the vertical particle velocity,  $St \equiv \tau_p/\tau$  is the Stokes number,  $Sv \equiv \tau_p g/u_\tau$  is the settling number, and we may also write  $Sv = St/Fr$ , where  $Fr \equiv u_\tau/\tau g$  is the Froude number. Gravitational settling directly affects the spatial distribution  $\varrho$  through the contribution  $Sv$  in (2.2). It also indirectly

affects  $\varrho$ , because  $\langle u^p(t) \rangle_z$  and  $S$  are affected through the way that settling modifies how the particles interact with the turbulent flow.

The first two terms on the rhs of (2.2) are positive near the wall (Johnson *et al.* 2020; Bragg *et al.* 2020). The first describes a diffusive velocity that arises from decoupling between the particle velocity and the local fluid velocity. The second term involves a velocity  $\langle u^p(t) \rangle_z$  that arises from the particles preferentially sampling the underlying turbulent flow, that vanishes for fully-mixed fluid particles (Bragg *et al.* 2012). The third term involves the turbophoretic velocity  $St\nabla_z S$  that arises due to inhomogeneities in the turbulence and particle inertia (Reeks 1983), and the fourth is the Stokes gravitational settling velocity. Detailed explanations of each of the terms in (2.2) may be found in Bragg *et al.* (2020).

Equation (2.2) is regularly perturbed with respect to  $Sv$ , i.e. the limit of (2.2) for  $Sv \rightarrow 0$  is equal to (2.2) with  $Sv = 0$ . This would suggest that for sufficiently small  $Sv$  the effect of gravity must vanish. However, since both gravitational settling and the turbophoretic velocity contribute to the drift mechanism that drives the particles towards the wall, the importance of gravitational settling cannot be determined simply by considering  $Sv$ . Indeed,  $Sv \ll 1$  cannot be used as a criteria for neglecting gravitational settling because for the same parameters we may also have  $St|\nabla_z S| \ll 1$ . Instead, the dynamical significance of gravitational settling is to be determined by comparing it to the turbophoretic velocity through the quantity

$$\Psi \equiv Sv/St|\nabla_z S| = 1/(Fr|\nabla_z S|). \quad (2.3)$$

Only if  $\Psi \ll 1$  can gravitational settling be ignored, and therefore, while some previous studies have argued that gravity can be neglected if  $Sv \ll 1$ , this need not be the case because  $\Psi$  may be  $\geq O(1)$  even when  $Sv \ll 1$ . We will now consider the behavior of  $\Psi$  in order to determine when gravitational settling may be neglected.

In the regime  $St \ll 1$ ,  $S = \langle uu \rangle + O(St)$  (Johnson *et al.* 2020), where  $\langle uu \rangle$  is the wall-normal fluid Reynolds stress. For small  $z$ , we have  $S \sim az^4$  (where  $a$  is non-dimensional and independent of  $z$ ) and hence

$$\Psi \sim 1/(4Fra z^3), \quad \text{for } St \ll 1, z \ll 1. \quad (2.4)$$

This shows that unless  $Fr \rightarrow \infty$ , there will always exist a range of  $z$  near the wall where  $\Psi \geq O(1)$ . Therefore, in the near-wall region, gravitational settling can play a leading order role on the particle dynamics, even if  $Sv \ll 1$ . It is also important and interesting to note that in the regime  $St \ll 1$ ,  $\Psi$  is independent of  $St$ .

For  $St \geq O(1)$  and  $z \ll 1$ ,  $S$  behaves as a power law in  $z$  with a  $St$  dependent exponent (Sikovsky 2014), i.e.  $S \sim bz^\xi$ , where  $\xi(St) \in [0, 4]$ . In this case we have

$$\Psi \sim 1/(\xi Fr b z^{\xi-1}), \quad \text{for } St \geq O(1), z \ll 1. \quad (2.5)$$

This again shows that unless  $Fr \rightarrow \infty$ , there will always exist a range of  $z$  near the wall where  $\Psi \geq O(1)$  if  $\xi > 1$ . For  $\xi < 1$ ,  $\lim_{z \rightarrow 0} \Psi \rightarrow 0$ , showing that in this case gravitational settling becomes negligible as the wall is approached. The regime  $\xi < 1$  corresponds to the case where the particles are moving almost ballistically towards the wall and the turbophoretic velocity overwhelms the Stokes settling velocity.

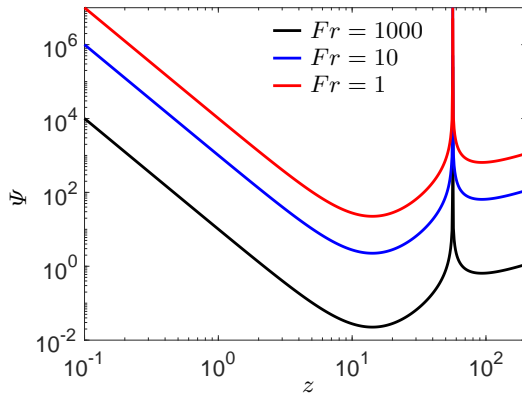


Figure 1: Plot of  $\Psi$  as a function of  $z$  for various  $Fr$ .

To consider the behavior outside of the regime  $z \gg 1$ , we may consider the behavior of  $\Psi$  for  $St \ll 1$  using curve fit data for  $\langle uu \rangle$  from [Kallio & Reeks \(1989\)](#), since  $S = \langle uu \rangle + O(St)$  for  $St \ll 1$  ([Johnson et al. 2020](#)). Plots of the resulting form for  $\Psi$  are shown in figure 1, and reveal that the behavior predicted in (2.4) applies up to  $z = O(10)$ , due to the fact that the behavior  $\langle uu \rangle \sim az^4$  works well up to  $z = O(10)$ , even though only formally valid for  $z \ll 1$ . Even for a case with very weak gravity, e.g.  $Fr = 1 \times 10^3$ ,  $\Psi$  is  $\geq O(1)$  throughout much of the boundary layer, showing that the effect of gravity cannot be ignored, despite the fact that  $Sv = St/(1 \times 10^3)$  for this case, i.e. very small for typical values of  $St$ .

For  $St \geq O(1)$ , the behavior of  $S$  is unknown outside of the regime  $z \ll 1$  and therefore the behavior of  $\Psi$  cannot be described analytically for this regime. However, we will consider this using our DNS data.

The considerations in this section therefore suggest that the effect of gravity on particle transport in a turbulent boundary layer can be strong even when  $Sv \ll 1$ . We now turn to use DNS to explore the problem in more detail, and to see the quantitative effects of gravitational settling on the spatial distribution  $\varrho$  in regimes where  $Sv \ll 1$ .

### 3. Direct Numerical Simulations

#### 3.1. Equations of motion

DNS is used to solve the incompressible Navier-Stokes equations, which are then used in a one-way coupled scenario to solve for the motion of heavy, inertial, point-particles that are subject to drag and gravitational forces. We refer to [Bragg et al. \(2020\)](#) for details on the method. Note that as in that paper, we also add a diffusion term when solving for the particle position

$$d\mathbf{x}^p(t) = dt\mathbf{v}^p(t) + \sqrt{2\kappa dt}d\boldsymbol{\xi}(t), \quad (3.1)$$

where  $\mathbf{x}^p(t)$ ,  $\mathbf{v}^p(t)$  are the particle position and velocity, and  $\kappa$  is a constant diffusion coefficient. The term  $d\boldsymbol{\xi}(t)$  is a normalized vector-valued Wiener process with unit variance. In the absence of this term, gravity can lead to very large near-wall particle concentrations, and very long simulation times are required for the system to attain the state where the vertical particle mass flux is zero. Adding the diffusion term alleviates this problem by suppressing the growth of the near-wall particle concentration. The particle motion behaves the same as the system with  $\kappa = 0$  down to a distance from the wall

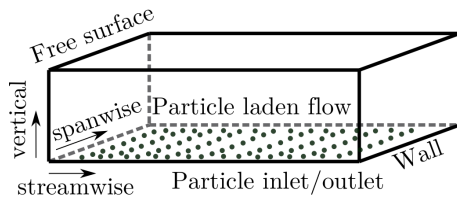


Figure 2: The particle concentration is held constant using a reservoir at the wall.

$\delta_\kappa$  that is controlled by  $\kappa$ , below which the diffusion term dominates and suppresses the growth of the particle concentration. For our choice of  $\kappa$  (see below), we find  $\delta_\kappa = O(1)$ .

### 3.2. Boundary conditions and numerical parameters

We solve the flow at  $Re_\tau = 315$ , using a constant pressure gradient to force the flow. The streamwise  $x$  and spanwise  $y$  directions are periodic, and the wall at  $z = 0$  imposes a no-slip condition on the fluid velocity field. At the upper wall,  $z = H$ , a free-slip (i.e., zero-stress) condition is imposed on the fluid velocity. This setup provides a canonical case of wall-bounded turbulence; figure 2 provides a schematic of the configuration.

A constant number concentration of particles is maintained in a reservoir just beneath the wall at  $z = 0$ , while at the upper domain boundary  $z = H$ , the particles rebound elastically, producing a zero mass-flux configuration. For the diffusion term in (3.1) we set  $\kappa = \nu/100$ , where  $\nu$  is the fluid kinematic viscosity. This value is large enough to enable particles to be efficiently suspended into the flow from the reservoir and to enable the particle statistics to reach steady-state in a reasonable amount of time, while also being small enough so that the diffusion term only significantly impacts the particle motion very close to the wall ( $z < O(1)$ ).

We simulate four different Stokes numbers  $St = 3 \times 10^{-3}, 0.93, 9.30, 46.5$ , and for each of these we consider  $Sv = 0, 3 \times 10^{-3}$  and  $2.5 \times 10^{-2}$ . In order to maintain a constant  $Sv$  while varying  $St$ , the gravitational acceleration  $g$  is varied.

## 4. Results & Discussion

We begin by considering in figure 3 the results for the spatial distribution  $\varrho$  for different  $Sv$  and  $St$ . For  $Sv = 3 \times 10^{-3}$ , the results show that throughout much of the boundary layer, gravitational settling is unimportant as observed by the overlap with the  $Sv = 0$  case. However, closer to the wall, it is seen that gravitational settling enhances the particle concentration by as much as a factor of two, despite the fact that  $Sv$  is very small. For  $Sv = 2.5 \times 10^{-2}$ , gravitational settling is seen to have a very strong impact on  $\varrho$ , leading to enhancements of the near wall concentration (relative to the bulk) of several orders of magnitude in some cases. Note that due to the inclusion of the diffusion term in (3.1), the concentration profile plateaus as the wall is approached, whereas in the absence of this term it would continue to grow as  $z$  decreases. Therefore, the effect of gravitational settling enhancing the near wall concentration would be even stronger in the absence of the diffusion term.

The strong effect of gravitational settling even when  $Sv$  is very small was explained in §2 as being due to the fact that the dynamical significance of gravitational settling is determined by its strength compared with the turbophoretic velocity, as quantified by  $\Psi$ , and not by its size compared with  $u_\tau$ , which would be quantified using  $Sv$ . In figure 4 we plot the results for  $\Psi$  computed from the DNS, for various  $St$  and  $Sv$ . For  $St \geq 0.93$ , the results show that when  $Sv = 3 \times 10^{-3}$ ,  $\Psi \ll 1$  throughout much of

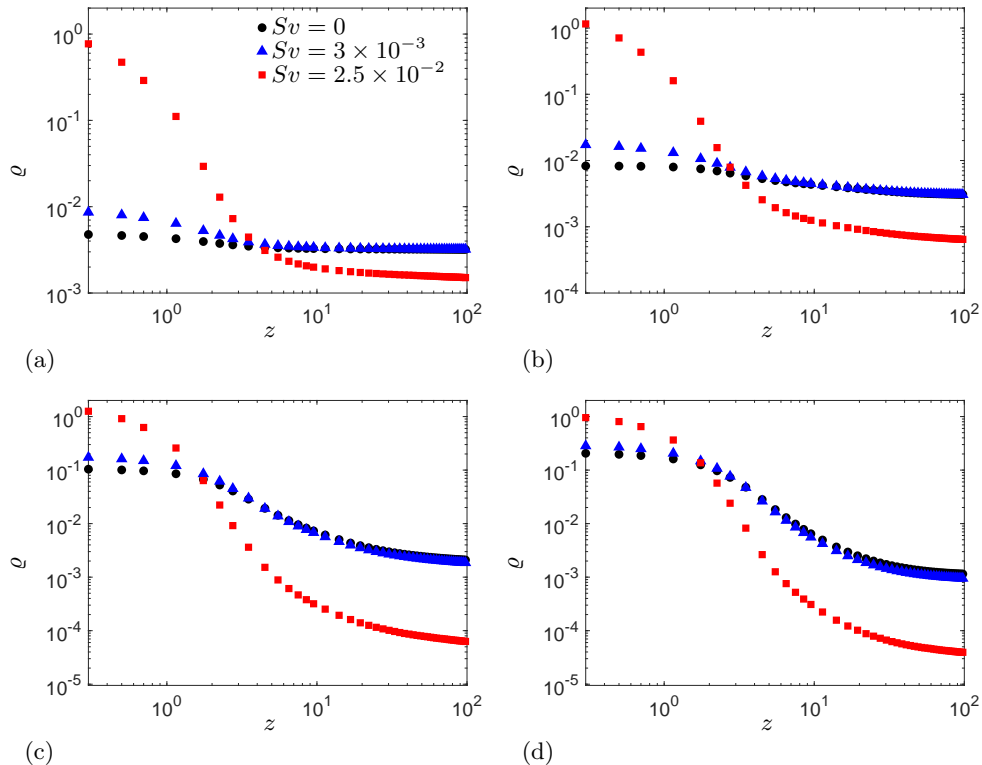
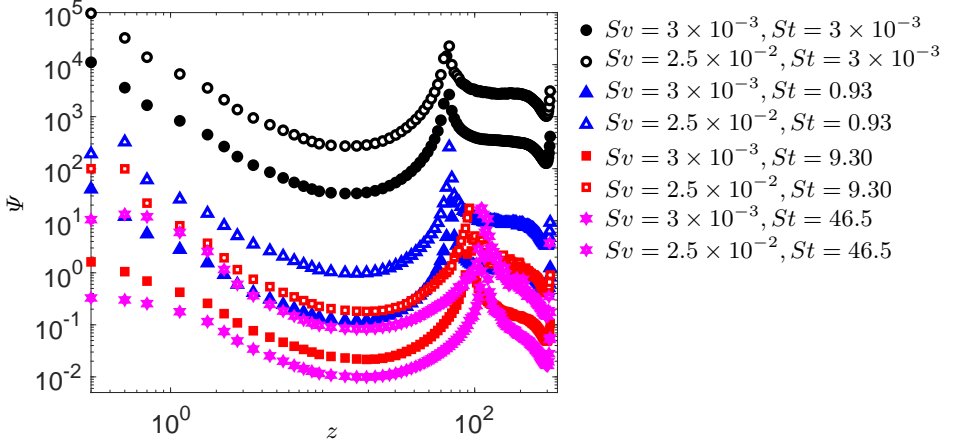
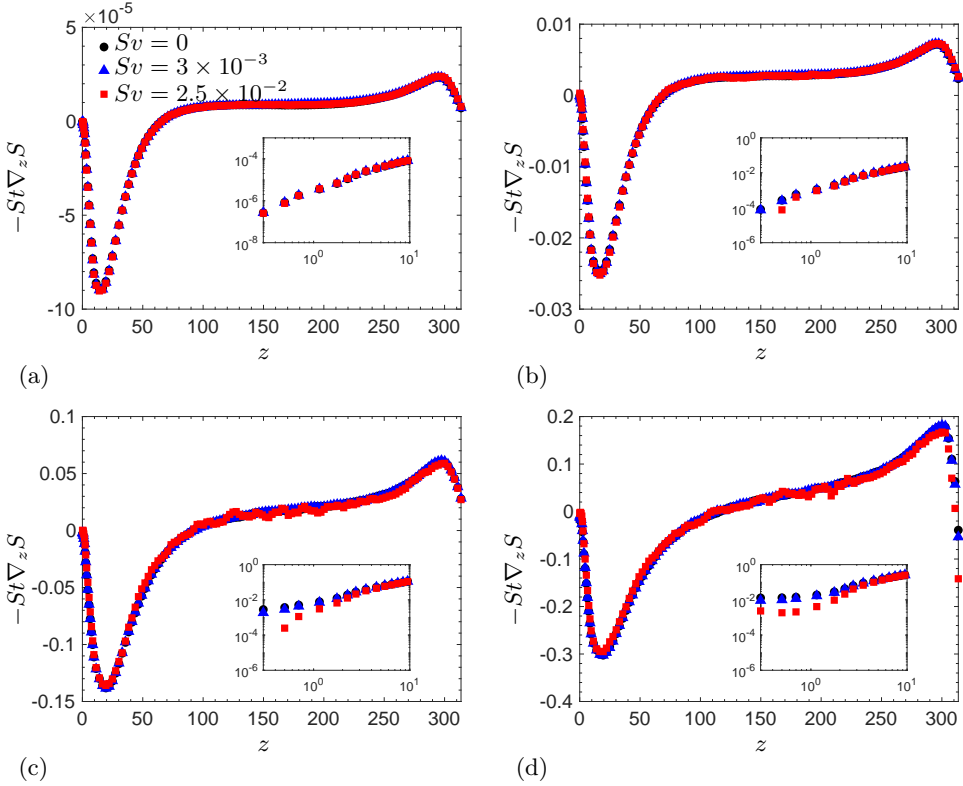


Figure 3: Plot of  $\rho$  as a function of  $z$  for different  $Sv$ , and (a)  $St = 3 \times 10^{-3}$ , (b)  $St = 0.93$ , (c)  $St = 9.30$ , (d)  $St = 46.5$ .

the boundary layer, but  $\Psi \geq O(1)$  can occur close to the wall. This corresponds to the results in figure 3 that showed that for  $Sv = 3 \times 10^{-3}$ , the effect of gravitational settling is negligible, except close to the wall where it can enhance the particle concentration. When  $Sv = 2.5 \times 10^{-2}$ ,  $\Psi$  can become much greater than one, indicating a leading order role being played by gravitational settling. For  $St = 3 \times 10^{-3}$ ,  $\Psi$  is very large for both  $Sv$  numbers considered, indicating a very strong contribution from gravitational settling (although the concentration profiles for these cases are, however, only weakly inhomogeneous since the actual drift velocities producing the inhomogeneities are small compared with the contribution  $\rho \langle u^p(t) \rangle_z$  that drives the particles away from the wall; see equation (2.2)).

We now turn to consider how gravitational settling affects each of the mechanisms governing  $\rho$  according to equation (2.2). In figure 5 we show the results for the turbophoretic drift velocity  $-St \nabla_z S$  for different  $St$  and  $Sv$ . For  $St \leq O(1)$  we find that  $-St \nabla_z S$  is almost independent of  $Sv$  for the values of  $Sv$  considered. For  $St > O(1)$ ,  $-St \nabla_z S$  is insensitive to  $Sv$  for  $z \geq O(10)$ , but decreases with increasing  $Sv$  for  $z \leq O(1)$ . This reduction with increasing  $Sv$  corresponds to a decrease in the magnitude of  $S$ , and can be explained as follows.

Figure 4: DNS data for  $\Psi$  as a function of  $z$  for different  $Sv$  and  $St$ .Figure 5: Plots of the turbophoretic velocity  $-St\nabla_z S$  as a function of  $z$  for different  $Sv$ , and (a)  $St = 3 \times 10^{-3}$ , (b)  $St = 0.93$ , (c)  $St = 9.30$ , (d)  $St = 46.5$ . The insets correspond to the same plots (except that the vertical axis is now  $St\nabla_z S$ ) but in a log-log scale to highlight the behavior for small  $z$ .

Particle inertia enables the particles to retain a memory of their interaction with the turbulent flow at locations further away from the wall, and close to the wall this causes their velocities to exceed the local velocities of the fluid. However, gravity reduces the correlation timescale of the flow seen by the particle by causing them to fall through the flow (Csanady 1973), which in turn reduces the ability of the particles to be influenced by their interaction with the turbulence along their path-history. As a result, the inertial particle velocities begin to be dominated more and more by their interaction with the local flow, and inertia modulates the particle response to the local flow. This then causes their velocity fluctuations to be smaller than those of the local fluid as  $Sv$  is increased (This is analogous to the effect of settling on the collision velocities of inertial particles in turbulence, see Ireland *et al.* (2016)). The reduction in  $-St\nabla_z S$  as  $Sv$  is increased is, however, smaller than the increase in  $Sv$ , so that the overall drift velocity driving the particles towards the wall, namely  $-St\nabla_z S - Sv$ , becomes larger in magnitude as  $Sv$  is increased.

Another implication of this is that since  $-St\nabla_z S$  reduces in magnitude as  $Sv$  is increased, then while the quantity  $\Psi \equiv Sv/St|\nabla_z S|$  behaves as  $\Psi \propto Sv$  for  $St \ll 1$ , for  $St \geq O(1)$ ,  $\Psi$  increases with increasing  $Sv$  faster than  $\Psi \propto Sv$ .

In figure 6 we show the results for the averaged fluid velocity sampled by the particles,  $\langle u^p(t) \rangle_z$ , for different  $St$  and  $Sv$ . In striking contrast to the results just considered for  $-St\nabla_z S$ , we find that  $\langle u^p(t) \rangle_z$  is strongly dependent upon  $Sv$  when  $St$  is small, and in particular,  $\langle u^p(t) \rangle_z$  increases significantly as  $Sv$  is increased. This can be explained as follows: As shown in Zaichik (1999), under the assumption that the fluid velocity field has Gaussian statistics we may obtain

$$\langle u^p(t) \rangle_z \approx -\frac{\tau_L \langle uu \rangle}{1 + St/\tau_L} \nabla_z \varrho. \quad (4.1)$$

While the Gaussian assumption may in general break down, in Sikovsky (2014) it was shown that due to the scaling of the fluid velocity field with  $z$  near the wall, (4.1) captures the leading order behavior in the near-wall region. Using this approximation in (2.2) we obtain

$$0 \approx -StS\nabla_z \varrho - \frac{\tau_L \langle uu \rangle}{1 + St/\tau_L} \nabla_z \varrho - St\varrho\nabla_z S - Sv\varrho. \quad (4.2)$$

As discussed earlier, in the regime  $St \ll 1$ ,  $S = \langle uu \rangle + O(St)$ , and so in this regime (4.2) reduces to leading order in  $St$  to

$$0 \approx -\tau_L \langle uu \rangle \nabla_z \varrho - St\varrho \nabla_z \langle uu \rangle - Sv\varrho, \quad (4.3)$$

and if  $\Psi \gg 1$  this further reduces to

$$0 \approx -\tau_L \langle uu \rangle \nabla_z \varrho - Sv\varrho. \quad (4.4)$$

Recalling that  $-\tau_L \langle uu \rangle \nabla_z \varrho$  is the approximation to  $\langle u^p(t) \rangle_z$  for  $St \ll 1$ , then we see that for  $St \ll 1$ ,  $\langle u^p(t) \rangle_z$  must increase with increasing  $Sv$ , as observed in figure 6 (very close to the wall, (4.4) breaks down since it ignores the diffusion contribution associated with  $\kappa$ ). Physically, this reflects the fact that as  $Sv$  is increased, since the drift velocity driving the particles towards the wall becomes stronger, the particles must preferentially sample upward moving regions of the flow more strongly in order to satisfy the zero mass-flux condition. In a turbulent boundary layer, the upward moving regions are associated with ejection events, and these results then imply that for  $St \ll 1$ , the way the inertial particles interact with the near-wall structures of the turbulent flow is profoundly affected by gravity, even when  $Sv$  is small, and in particular, that gravity leads the particles to

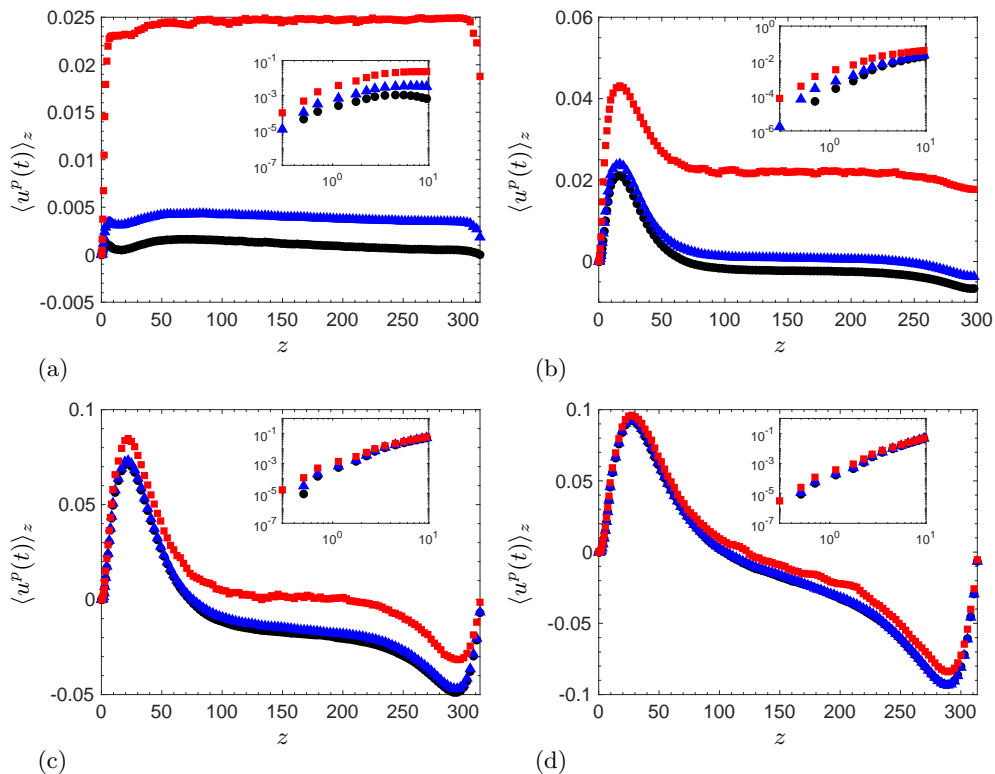


Figure 6: Plots of the average fluid velocity sampled by the particles  $\langle u^P(t) \rangle_z$  as a function of  $z$  for different  $St$ , and (a)  $St = 3 \times 10^{-3}$ , (b)  $St = 0.93$ , (c)  $St = 9.30$ , (d)  $St = 46.5$ . The insets correspond to the same plots but in a log-log scale to highlight the behavior for small  $z$ . Legend is the same as in figure 5.

preferentially sample ejection events even more strongly than they do in the absence of gravity. We note, however, that this increase must eventually saturate because in the limit  $St \rightarrow \infty$ , the particles experience the fluid velocity field as a delta-correlated signal for which  $\langle u^P(t) \rangle_z = 0$  (see Bragg *et al.* (2020)).

## 5. Conclusions

We have considered the role of gravitational settling on the concentration profiles of small particles in wall-bounded turbulent flows. We provided theoretical arguments and DNS results that show that settling can play a leading order role in determining the concentrations, even when the Stokes settling velocity is very small compared with the fluid friction velocity. The reason is that the dynamical relevance of settling is determined by the size of the Stokes settling velocity compared with the turbophoretic velocity, not compared with the fluid friction velocity (or any other fluid velocity scale). While our results are for particles experiencing a Stokes drag force, the same arguments would apply even for particles experiencing non-linear drag forces, except that the Stokes settling velocity would be replaced with that based on the average particle response time.

One practical issue is that it is not always possible to reliably predict the turbophoretic

velocity *a priori*, and therefore when performing numerical simulations, it may not be clear whether the parameter regime considered justifies neglecting particle settling. Our results suggest that it is probably best to always retain the particle settling, and then one can check *a posteriori* whether the settling plays any important role.

## Acknowledgements

The authors acknowledge computational resources provided by the High Performance Computing Modernization Program (HPCMP), and by the Center for Research Computing (CRC) at the University of Notre Dame. DR acknowledges grant G00003613-ArmyW911NF-17-0366 from the US Army Research Office.

## Declaration of Interests

The authors report no conflict of interest.

## REFERENCES

- BALACHANDAR, S. 2009 A scaling analysis for point particle approaches to turbulent multiphase flows. *Int. J. Multiph. Flow* **35** (9), 801 – 810, special Issue: Point-Particle Model for Disperse Turbulent Flows.
- BRAGG, A., SWAILES, D. C. & SKARTLIEN, R. 2012 Drift-free kinetic equations for turbulent dispersion. *Phys. Rev. E* **86**, 056306.
- BRAGG, A. D., RICHTER, D. H. & WANG, G. 2020 Mechanisms governing the settling velocities and spatial distributions of inertial particles in wall-bounded turbulence. *arXiv preprint arXiv:2010.02674* .
- CHAMECKI, M., MENEVEAU, C. & PARLANGE, M. B. 2009 Large eddy simulation of pollen transport in the atmospheric boundary layer. *J. of Aerosol Sci.* **40**, 241–255.
- CSANADY, G. T. 1973 *Turbulent Diffusion in the Environment*. Reidel, Boston.
- IRELAND, P. J., BRAGG, A. D. & COLLINS, L. R. 2016 The effect of reynolds number on inertial particle dynamics in isotropic turbulence. part 2. simulations with gravitational effects. *Journal of Fluid Mechanics* **796**, 659–711.
- JOHNSON, P. L., BASSENNE, M. & MOIN, P. 2020 Turbophoresis of small inertial particles: theoretical considerations and application to wall-modelled large-eddy simulations. *J. Fluid. Mech.* **883**, A27.
- KALLIO, G. A. & REEKS, M. W. 1989 A numerical simulation of particle deposition in turbulent boundary layers. *Int. J. Multiphase Flow* **15**, 433.
- MAXEY, M. R. 1987 The gravitational settling of aerosol particles in homogeneous turbulence and random flow fields. *J. Fluid Mech.* **174**, 441–465.
- MAXEY, M. R. & RILEY, J. J. 1983 Equation of motion for a small rigid sphere in a nonuniform flow. *Phys. Fluids* **26**, 883–889.
- REEKS, M. W. 1983 The transport of discrete particles in inhomogeneous turbulence. *J. Aerosol Sci.* **14** (6), 729–739.
- RICHTER, D. H. & CHAMECKI, M. 2018 Inertial effects on the vertical transport of suspended particles in a turbulent boundary layer. *Bound.-Layer Meteorol.* **167**, 235–256.
- ROUSE, H. 1937 Modern conceptions of the mechanics of turbulence. *Trans. Am. Soc. Civ. Eng.* **102**, 463–505.
- SIKOVSKY, D. P. 2014 Singularity of inertial particle concentration in the viscous sublayer of wall-bounded turbulent flows. *Flow Turbul Combust* **92**.
- SOLDATI, A. & MARCHIOLI, C. 2009 Physics and modelling of turbulent particle deposition and entrainment: Review of a systematic study. *Int. J. Multiphase Flow* **35**, 827–839.
- ZAICHIK, L. I. 1999 A statistical model of particle transport and heat transfer in turbulent shear flows. *Phys. Fluids* **11** (6), 1521–1534.